AIChE

Analysis of Stirred Tanks with Two-Zone Models

Ville Alopaeus
Faculty of Chemistry and Materials Science, Dept. of Biotechnology and Chemical Technology, Helsinki University of Technology, Espoo, Finland

Pasi Moilanen
Process Flow Oy, Tampere, Finland

Marko Laakkonen
Neste Jacobs Oy, Porvoo, Finland

DOI 10.1002/aic.11850
Published online August 26, 2009 in Wiley InterScience (www.interscience.wiley.com).

Stirred tank turbulence and fluid flow characteristics are analyzed based on a two-zone model. Instead of using the zonal model for stirred tank performance prediction as often proposed in the literature, the zoning is used here as a tool for mixing analysis. A systematic zoning approach is proposed, where the tank is divided into two nested regions. By gradually increasing the inner zone volume, continuous curves can be obtained for turbulent energy dissipation distribution and pumping numbers between the zones as functions of the zone sizes. It is shown here that these curves can be used as a powerful tool for visualizing stirred tank performance. They can be used, e.g., in impeller performance comparisons and analysis of mixing characteristics with changing rheology, or to examine various numerical aspects related to stirred tank CFD modeling. © 2009 American Institute of Chemical Engineers *AIChE J,* 55: 2545–2552, 2009
Keywords: zonal modeling, stirred tanks, CFD, mixing

Introduction

Modeling of local conditions in stirred tanks is of fundamental importance, especially in cases where the tank performance is dictated by physical phenomena whose time scales are shorter than the vessel mixing time. Most notably, the impeller region has typically an order of magnitude higher turbulent energy dissipation than the bulk region. This is important when dealing with mass transfer or chemical kinetics.

In the past, this need has been addressed by various modeling approaches. In the simplest ones, the tank is divided in just two sections: the impeller and the bulk regions. A further improvement can be made by dividing the tank into several regions that are separately assumed completely mixed. Connections between these regions can be obtained by computational fluid dynamics (CFD) modeling or by measurements.

Accurate calculation of the most important fluid flow parameters, namely fluid velocity, turbulent kinetic energy, turbulent energy dissipation, and pressure gradients, usually requires more CFD control volumes than a satisfactory simulation of chemical concentrations or reaction kinetics. An attractive approach would then be either calculating flow patterns with CFD or by measuring the flow patterns directly. Then actual reactor performance with chemical and mass transfer rate models can be predicted with a simpler block, or zone, models. This approach has also been successfully applied in the past.[1–10]

Correspondence concerning this article should be addressed to V. Alopaeus at ville.alopaeus@tkk.fi

In this contribution, we take advantage of the simplest zonal models, namely the two-zone models, from a different perspective. The models are not just analyzed based on their capability to predict some stirred tank performance characteristics, but rather these simple models are used as a new and illustrative tool for visualizing the most important mixing properties of various tank configurations. Furthermore, the results that can be obtained from these simple zone models introduce a new way to verify CFD results and compare various computational grids and numerical schemes.

An important practical aspect in stirred tank reactor design is the choice of tank geometry and particularly selection of appropriate impeller type. There are numerous impeller selection guidelines available in the literature.[11–13] The proposed analysis with two-zone models could give valuable insight into the selection process by offering a simple way of visualizing mixing characteristics of various configurations. These advantages are discussed in the following sections.

Zonal Modeling

In this work, we analyze some of the simplest zone models, most notably those where the tank is divided only in two nested zones. This kind of two-zone modeling can be used as a first step toward realistic description of fluid flow within stirred tanks, and indeed it has been used for it in the past, although not with such a systematic manner as proposed here.[14,15]

The most important variables describing mixing within the zones are as follows: (1) distribution of turbulent energy dissipation between the zones and (2) pumping numbers between the zones, describing the flow rate at the zones boundary. By gradually increasing the inner zone volume, a continuous pumping number curve can be obtained, describing the material exchange between the inner and outer zones for any zoning generated by the present approach. Another continuous curve can be similarly obtained for the average turbulent dissipation distribution between the zones. These curves represent one-dimensional projections of the three-dimensional turbulent energy dissipation and fluid flow fields in the tank. Tank division for the zoning is illustrated in Figure 1.

By defining a scalar parameter λ in such a manner that it assumes a value of zero when the smaller zone is just the impeller swept volume, and approaches one as the smaller volume simultaneously coincides the tank total volume at each direction, the tank can be divided into these two regions in a unique manner. Other methods of division, e.g., those based on some flow variables such as turbulence levels, could be used as well, but they would produce a division which is case dependent, making comparison and analysis of the figures more unclear. Note that the zone volume is proportional to the third power of λ.

There are two, perhaps even more useful, results from the present zoning scheme. The first result is that the proposed zoning brings us a new and simple tool for analyzing stirred tank operation by giving us two simple graphs that can be used for easily comprehendible visualization of fluid flow and turbulence characteristics. This visualization can be used for improved understanding of mixing during stirred tank design and impeller selection. The second result from the zoning is a new method for analyzing CFD result quality.

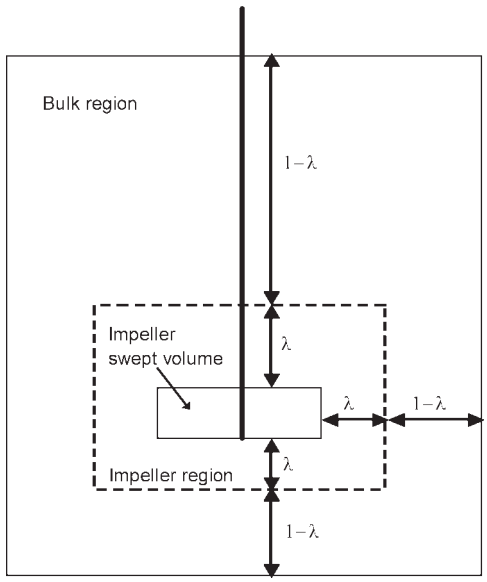

Figure 1. Zoning of a stirred tank.

When $\lambda = 0$, impeller region coincides with the impeller swept volume, and when $\lambda = 1$, impeller region encompasses the whole tank.

Results and Discussion

In this work, several CFD cases were calculated with CFX 5.7 software, and analyzed based on the zoning scheme. All simulations were carried out in a steady-state mode using the multiple frames of reference-approach for impeller modeling and Reynolds averaged Navier-Stokes (RANS) equations as material and momentum balances. This approach was chosen because it is widely used and is a reasonable compromise between computational speed and result accuracy. For the Rushton turbine cases, the mesh was structured and evenly divided. The impeller type test simulations were carried out with unstructured meshes due to complex impeller geometries. Average flow rate between the zones were calculated in each case (average flow rate from outer-to-inner and inner-to-outer zones). Naturally these flow rates should be equal at steady state, but for numerical reasons there may be small discrepancies in instantaneous values.

First we carried out one phase mixing simulations with varying tank size and impeller speed to confirm that the zonal models based on pumping numbers are scale and impeller speed invariant (Table 1, Cases 1–4), as indicated in our earlier work.[5] Then we analyzed numerical issues such as CFD grid size (spatial resolution), discretization method and turbulence model (Cases 5–10), rheological effects with non-Newtonian (viscous shear-thinning) liquids (Cases 11–14), and finally the impeller type with simulations carried out for gas–liquid system[16] (Cases 15–17). These cases were chosen so that first a well-known test case was modeled to study numerical issues (pure water, standard tank with a Rushton turbine). Then some industrially more

Table 1. Simulated Cases

Case	Tested Effect	Tank Volume (dm^3)	Phases	Number of Global Grid Nodes in CFD	Discretization Type	Turbulence Model	Impeller Type	Agitation (W/kg) (Liquid)
1	Vessel size	14	Water	395,697	2nd order	k-ε	Rushton	2.97
2	Vessel size	20,000	Water	395,697	2nd order	k-ε	Rushton	2.97
3	Power input	194	Water	395,697	2nd order	k-ε	Rusthon	1.49
4	Power input	194	Water	395,697	2nd order	k-ε	Rushton	5.93
5	Grid size	194	Water	35,737	2nd order	k-ε	Rushton	2.97
6	Grid size	194	Water	120,794	2nd order	k-ε	Rushton	2.97
7	Grid size	194	Water	395,697	2nd order	k-ε	Rushton	2.97
8	Grid size	194	Water	761,425	2nd order	k-ε	Rushton	2.97
9	Discretization method	194	Water	395,697	1st order	k-ε	Rushton	2.97
10	Turbulence model	194	Water	395,697	2nd order	SST	Rushton	2.97
11	Rheology	194	0.25 wt % aq. xanthan	395,697	2nd order	SST	Rushton	2.97
12	Rheology	194	0.75 wt % aq. xanthan	395,697	2nd order	SST	Rushton	2.97
13	Rheology	194	2.5 wt % aq. xanthan	395,697	2nd order	SST	Rushton	2.97
14	Rheology	194	4.0 wt % aq. xanthan	395,697	2nd order	SST	Rushton	2.97
15	Impeller type, phase	194	Water–air	120,794	2nd order	SST	Rushton	2.1
16	Impeller type, phase	194	Water–air	135,336	2nd order	SST	Combi-jet	2.1
17	Impeller type, phase	194	Water–air	154,568	2nd order	SST	Phase-jet	2.1

relevant cases were tested (non-Newtonian flow and a gas–liquid system with various impellers) to find out the potential of the model for real vessel and impeller analysis.

Standard tank geometry (diameter to liquid height ratio $D/H = 1$, bottom clearance 1/3 D, four baffles, and surface baffling) was used in all the simulated cases. Impeller to tank diameter ratio was 1/3 for the Rushton turbine, 0.46 for the Combijet, and 0.44 for the Phasejet impellers (the latter two were provided by Ekato). The base CFD case was simulation of a 200 dm^3 tank equipped with a Rushton turbine. In addition to the base case simulation with varying number of control volumes, we tested the scaling effect with additional vessel sizes of 14 dm^3, 20 m^3 (scale-up and scale-down), effect of impeller speed (power input), effect of three different impeller types, and effect of non-Newtonian fluid. The simulated cases are collected in Table 1. The simulated vessel was the same as used in our earlier CFD studies.[17,18]

Zoning curve interpretation and the scaling properties of the zonal models

The first test was related to the scale dependency of the two-zone model. For the purpose, we simulated three cases with different tank volumes. One was the base case, one with a smaller tank volume but with the same relative energy input as power/unit mass, and one with a larger tank volume and again with the same relative energy input. After that, we simulated two additional cases by changing power input from the base case but keeping the vessel size constant. The power input was changed so that first impeller speed was lowered to correspond half of the total power input compared to the base case, and then the impeller speed was increased to correspond twice the power input of the base case.

In Figure 2, zoning curves are shown for various vessel sizes and impeller speeds. Turbulent energy dissipation is scaled based on calculated vessel average in all cases shown in Figure 2. We can see that indeed the zone division according to the relative turbulent energy dissipation within the smaller of the two zones, and pumping number between the zones is scale and impeller speed independent. Impeller speed dependency is expected to be a valid assumption for fully turbulent tanks but before significant vortex formation or surface aeration starts to appear. The vessel size independent zoning is an expected, but nevertheless, highly advantageous feature of the model. As it can be further claimed that the size and the impeller speed independency is achieved irrespective to the inner zone size, this practically indicates that all zonal models based on pumping numbers between the zones are scale and impeller speed independent, not just the two-zone models used for the analysis here.

Some quite intriguing analysis can be carried out already from the curves shown in Figure 2. It can be seen that for the Rushton turbine, a lot of turbulent kinetic energy dissipates in the vicinity of the impeller. This is not a surprise, but presenting the data as one curve gives us a tool for rapid analysis of turbulence inhomogeneity within a stirred tank. It can be readily seen that within the impeller swept volume ($\lambda = 0$; impeller region volume $\sim$0.76% of the total tank volume), the estimated turbulent energy dissipation rate is $\sim$12 times higher than the vessel average. From the pumping number curve, we can see that as the smaller zone volume is increased, the exchange of material between the zones is increased up to a point where the zones are approximately

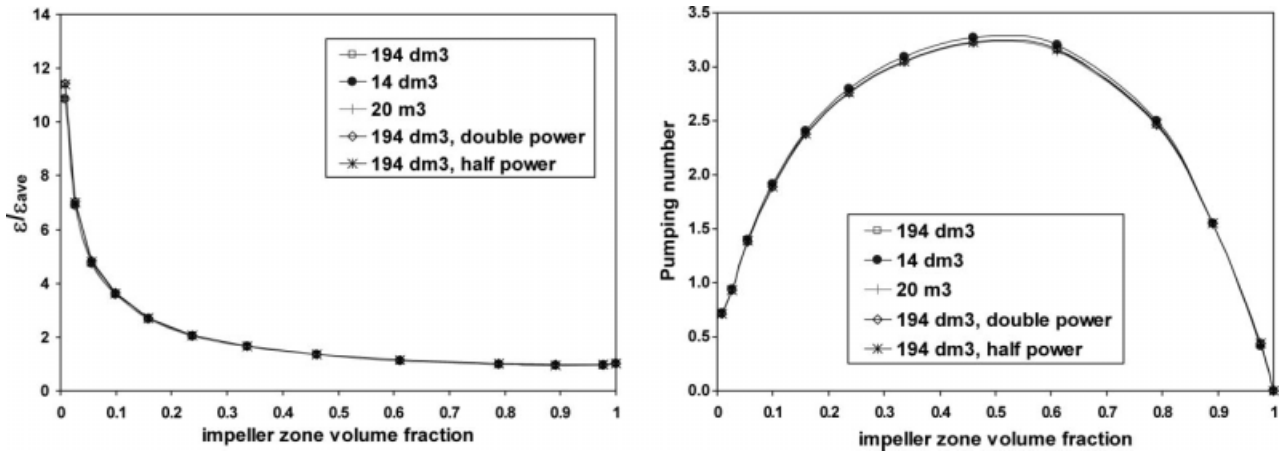

Figure 2. Zoning curves with different tank sizes.

Relative turbulent energy dissipation (left) and pumping number between the zones (right). Standard tank with rushton turbine, k-ε turbulence model.

equal in their volumes, and then the exchange decreases as the inner zone volume approaches the total tank volume. The leftmost point of the curve corresponds to the flow across the impeller swept volume, and is approximately equal to the traditional definition of the pumping number (although the pumping number is usually defined as the flow rate slightly outside the impeller tip).

Analysis of CFD results

Another possibility to exploit the zoning curves is in analysis of CFD results. They give much more information compared to that obtained by simply looking at the total power dissipation or impeller pumping number, yet the analysis can be carried out with a single glimpse. In Figure 3, results are shown for the base case with various computational grid densities. In Figure 4, discretization method and turbulence model effects are compared. The cases are shown in Table 2 along with calculated average power dissipation per unit mass. In Table 2, calculated turbulent energy dissipations are also compared to the measured one. It can be seen that coarse grids resolve only a small part of the turbulent dissipation (with 35,737 grid nodes only 10.8% of the total energy dissipated), and even with the finest grid tested (761,425 nodes) the calculated dissipation is slightly less than halve of the total energy input. No significant difference is observed between the SST and k-ε models except at the regions of highest turbulence dissipation, where SST predicts lower dissipation levels than k-ε. With the first-order discretization, the number of nodes needs to be considerably higher compared to the second-order discretization for any specified accuracy in turbulence modeling. By comparing Cases 6 and 9, it can be seen that with the first-order method the required number of nodes to predict a certain turbulent dissipation level (about 25% of the measured value) was approximately three times the number of nodes with the second-order discretization method.

Usually, CFD results are analyzed based on the predicted pumping number and the total energy dissipated via the turbulent mechanisms. It is well known that insufficient number

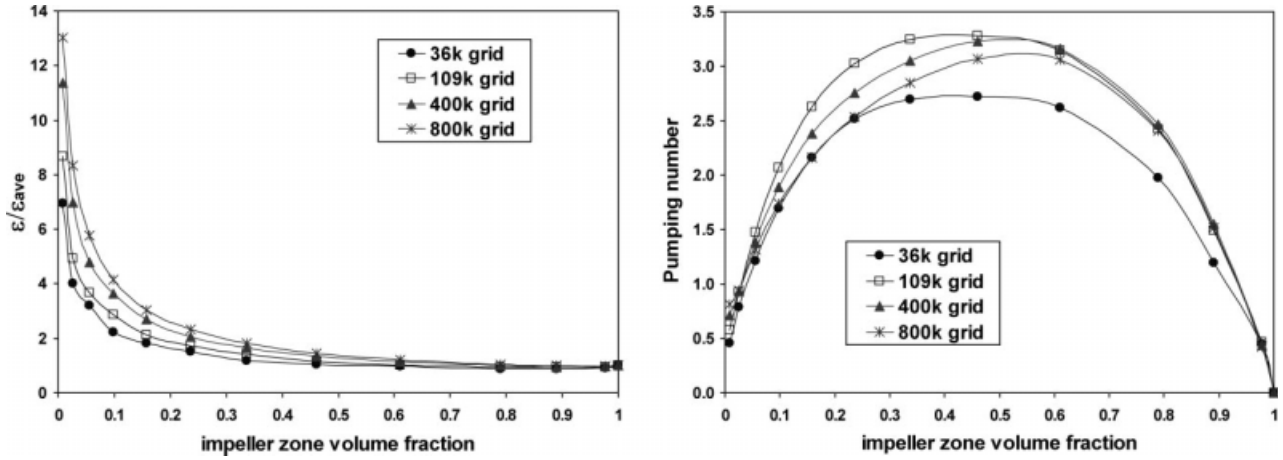

Figure 3. Zoning curves with various CFD grid resolutions.

Turbulent energy dissipation on the left and pumping numbers on the right.

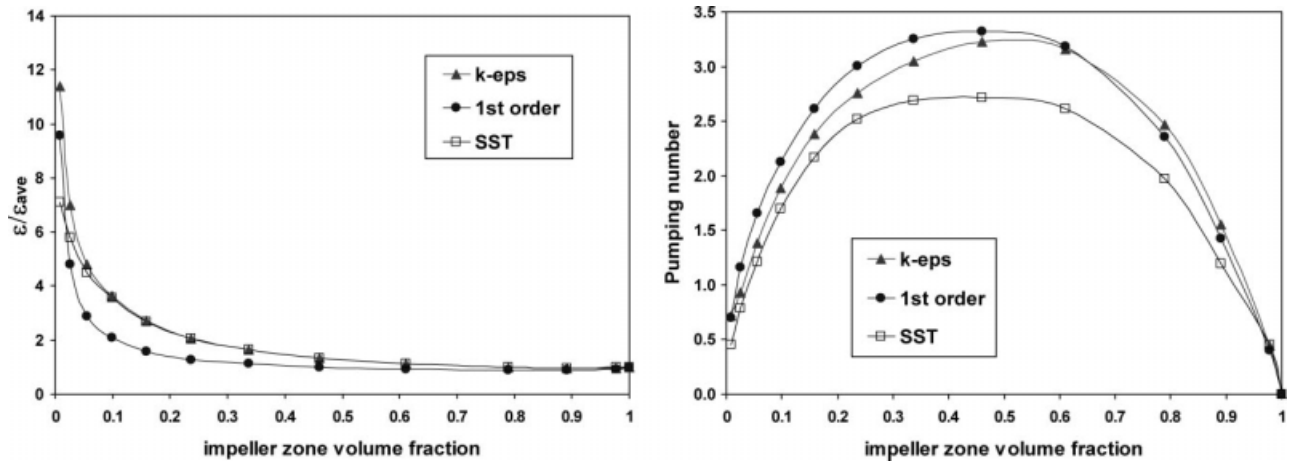

Figure 4. Effect of discretization order and turbulence model for the zoning curves with 400 k computational grid size.

of control volumes leads to under-predicted energy dissipation. Prediction of turbulent energy dissipation levels can also fail from other numerical reasons, such as steady-state calculation of inherently unsteady-state flow, or from inappropriate turbulence modeling, just to name a few. For such chemical and physical closure models that require accurate turbulence modeling, the first assumption is to scale the calculated turbulent energy dissipation field so that its integral corresponds to the measured power input, or if it is not known, a more accurate estimation calculated from the impeller torque obtained from the CFD results. This approach has been applied in the past.[6,16,17,19] However, when looking at Figure 3, it seems that this kind of linear scaling is not exactly correct but only a first approximation. Turbulence dissipation level is under predicted more severely near the impeller where turbulence levels are higher, compared to the more quiescent regions of the vessel. This suggests that a nonlinear scaling of turbulent dissipation should be applied, i.e., turbulent dissipation levels should be multiplied with larger scaling factors in regions where dissipation is higher and smaller scaling factors in the quiescent regions.

A plausible explanation for the curve shapes in Figure 3 is that a coarse grid cannot capture trailing vortices and other small-scale turbulent structures in the vicinity of the impeller. At impeller zone volume fractions of ~0.1–0.4, a coarse grid predicts that most of the kinetic energy remains at large flow structures, indicated by the pumping number, whereas the finer grids predict that the flow rates are hindered near the impeller, perhaps due to larger fraction of the kinetic energy dissipating via small-scale turbulent structures. This kind of analysis is much simpler with the proposed zoning curves than with the full 3D CFD simulation results. An additional interesting feature with the 800 k grid was that the CFD simulation did not fully converge to a steady-state solution, but rather had a slightly oscillatory solution. It is possible that there is a nonsteady state phenomenon with the finest grid, such as interaction between the impeller and the baffles, which is not yet resolved with the coarser grids. It is also surprising that there is still some grid dependency between 400 and 800 k grids despite relatively simple geometry.

Non-Newtonian fluids

Deviation from Newtonian behavior can appear in many ways, but common to non-Newtonian fluids is that their rheological properties strongly affect both the fluid flow pattern and the turbulence in stirred tanks. One of the most commonly encountered non-Newtonian behaviors is pseudoplasticity, where apparent viscosity decreases as shear rate is increased. This leads to relative increase of flow rates and mixing close to the impeller, and reduced mixing far from the impeller region. In most severe forms, this leads to cavern formation and completely stagnant regions within the stirred tanks when fluids with a yield stress are mixed. Although appropriate choice of impeller is important for mixing of Newtonian fluids, it is absolutely crucial for viscous non-Newtonian fluids. The zoning curves can be again used for the analysis of non-Newtonian fluid mixing and the appropriate choice of impellers.

In Figure 5, zoning curves are shown for five fluids with different viscosity characteristics. The reference case is water, and the other cases are 0.25, 0.75, 2.5, and 4.0 wt % xanthan solutions. Xanthan is a well-known compound that is produced in large amounts by fermentation in stirred

Table 2. Simulated Turbulent Energy Dissipations with Varying Grid Size, Discretization Method, and Turbulence Model

Case Number	Global Grid Nodes	Discretization Method Order, Turbulence Model	Calculated Power Dissipation (% of the Measured Value)
5	35,737	2nd, k-ε	0.32 W/kg (10.8%)
6	120,794	2nd, k-ε	0.69 W/kg (23.2%)
9	395,697	1st, k-ε	0.77 W/kg (25.9%)
7 (base)	395,697	2nd, k-ε	1.09 W/kg (36.6%)
10	395,697	2nd, SST	1.16 W/kg (39.1%)
8	761,425	2nd, k-ε	1.43 W/kg (48.1%)

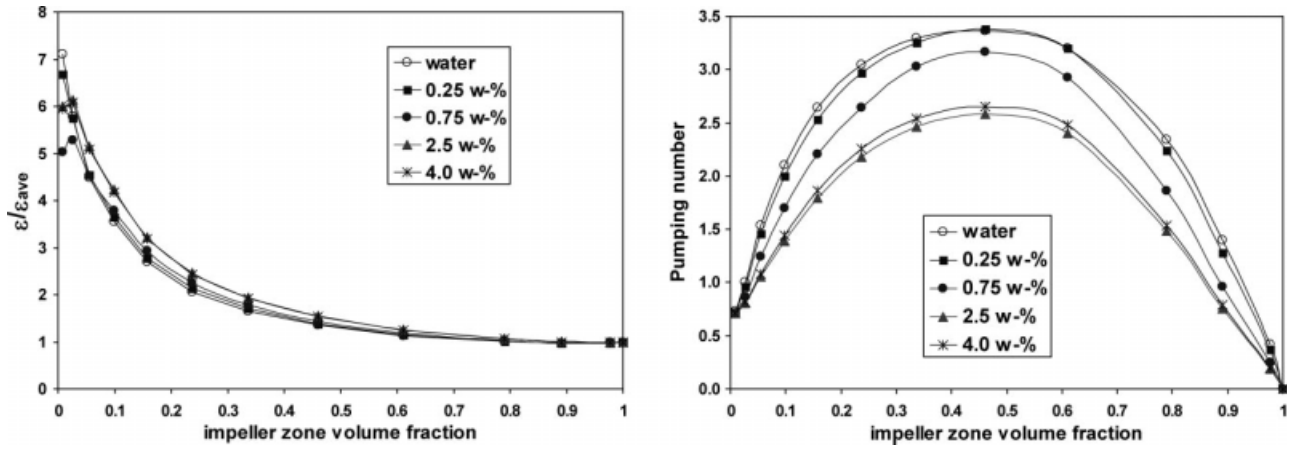

Figure 5. Zoning curves for some aqueous xanthan mixtures.

tanks. It possesses a pseudoplastic behavior, and its apparent viscosity is a strong function of concentration.[20] These results were calculated again with CFX 5.7, but now using SST model for turbulence. This was necessary due to large variations in turbulence levels, and especially due to almost laminar flow far away from the impeller region. The k-ε model predicted unphysical turbulence levels at the quiescent regions of the vessel in concentrated xanthan simulations.

It can be seen that as xanthan is added to the system, at first there is no significant change in fluid flow. As the xanthan concentration is increased above 0.25 wt %, the flow rates starts to decrease except very near the impeller tip, where pumping numbers remain at constant level due to unaltered impeller speed. Above 2.5 wt %, there is no further visible change in the zoning curves. In the turbulent energy dissipation curve, there is a noticeable change very near the impeller at the same xanthan concentrations where a change in the pumping number curve is observed. Interestingly, the turbulence dissipation near the impeller first decreases as the xanthan concentration is increased, but at high concentrations it is increased again. In general, differences between turbulent energy dissipation levels further away from the impeller are surprisingly small.

Zoning curves for various impellers

It is well known that various impellers possess very different mixing characteristics. Some impellers are designed for dispersion, with correspondingly high maximum turbulent energy dissipation. Other impellers are designed mainly for bulk mixing, or perhaps solids suspension. Optimal impellers for high gassing rates are usually different from those that can be used for low dispersed phase fraction liquid–liquid systems. Although there is a plethora of impeller selection guidelines for various mixing tasks, the zoning curves could be one further useful way of comparing various impeller types and understand the underlying differences between their dispersion and pumping characteristics. As an example, zoning curves for three different impellers are shown in Figure 6. The Rushton turbine is compared with Phasejet and Combijet impellers by Ekato in gas dispersion

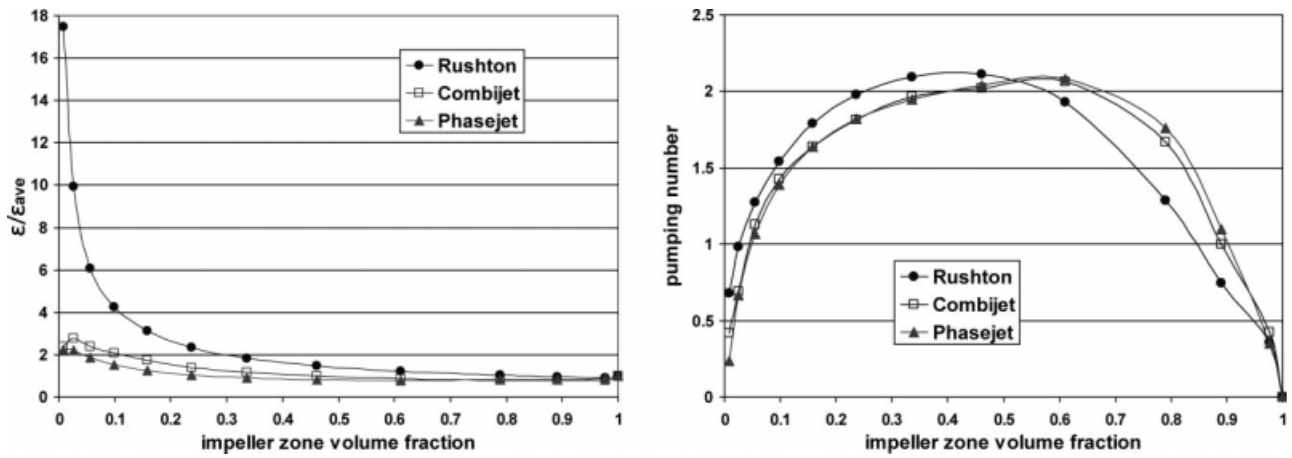

Figure 6. Zoning curves for three different impellers.

Two phase flow, SST turbulence model with 2.1 W/kg mixing power, and 0.7 vvm gassing rate.

conditions. In the examples shown here, the gassing rate is not particularly high so that the Rushton turbine case remains realistic (none of the impellers are flooded). The latter impellers are designed for gas dispersion at high gassing rates, and they do not suffer a dramatic drop in power number under heavy gassing as the Rushton turbine does. Further details of the simulated system can be found in Ref. [16]. In this comparison, the zoning always starts (i.e., $\lambda = 0$) from the impeller zone corresponding to the impeller swept volume by Rushton turbine.

From Figure 6, it can be seen that for the two impellers designed for gas dispersion at high gassing rates, the turbulent energy dissipation in the vicinity of the impeller is much lower than with the Rushton turbine. This is most probably a common feature for all impellers designed mainly for pumping action. Pumping numbers are also smaller for small impeller zone volumes, but higher for large impeller zone volumes. This indicates that mixing with Rushton turbine is not as effective further away from the impeller region as compared with the two other impellers.

It must be noted that for some impeller designs, e.g., anchor impellers, the zoning procedure should be modified. If we start from a smaller zone confined within the impeller swept region, the impeller zone would already accommodate considerable fraction of the total tank volume, and much of the relevant flow patterns would already be confined within the impeller zone. In those cases, it is necessary to reformulate the zoning, e.g., in such a way that the inner zone starts from the tip of the axis and grows then similarly as in the base case.

Future prospective

It is clear that the proposed zoning is only one possible way of obtaining the zoning curves. It is best suited for simulations of stirred tanks equipped with a single and relatively small impeller. In case of large impellers, the results would be most probably as illustrative as in the examples given here, but the zoning scheme should be modified so that the focus is also within the impeller swept volume. In cases of multiple impellers, it is possible to analyze each impeller separately with the present zoning, or combining all impellers into a single impeller zone composed of several spatially nonconnected volumes.

In cases of non-Newtonian fluids with severe cavern formation, more illustrative zoning curves could be obtained by modifying the zoning scheme so that the impeller zone reaches the cavern edges simultaneously in each direction. Then this point would also indicate cavern volume, and properties within and outside the cavern would be better represented in the curves. These alternative zoning schemes could be based on existing cavern models.[21]

The inherently time-dependent characteristics of mixing in stirred tanks can be represented by the proposed zoning curves by plotting a set of curves representing snapshot results of a time-dependent simulation. This article should be considered as a first step toward a new visualization technique related to stirred tank models.

Conclusions

A two-zone model for stirred tanks was proposed. The model is based on tank division into two nested regions in a systematic manner. By gradually increasing the inner zone volume, starting from the impeller swept volume and finally approaching the total tank volume, continuous curves are obtained for the most important factors characterizing small- and large-scale mixing. These are turbulent energy dissipation distribution and pumping numbers between the zones as functions of the zone sizes.

The zoning curves were analyzed for various test cases. Firstly, the well-known scaling property (scale independency) of the zonal modeling was verified and some general properties of the curves were discussed. Then the zoning curves were used for CFD result analysis. It was shown how grid dependency can be visualized for the whole tank instead of just using some characteristic integral properties of the numerically solved flow field. Then the effect of discretization scheme (first vs. second order discretization), and the choice of the turbulence model were visualized and discussed. After that, the zoning curves were used for analysis of non-Newtonian fluid mixing. Finally, some characteristics of various impellers in gas–liquid mixing operation were examined based on the zoning curves.

In all cases, the zoning curves revealed valuable information that can be used for deepening our knowledge of the mixing processes. They add up one prospective visualization technique to our set of tools for mixing operation analysis, with several potential application areas.

Acknowledgments

The authors would like to thank TEKES (Finnish Funding Agency for Technology and Innovation) for financial support.

Notation

D = tank diameter, m
D_{imp} = impeller diameter, m
H = liquid filled height of the tank, m
N = impeller speed, 1/s
N_p = pumping number, $N_p = Q/ND_{imp}^3$
Q = volumetric flow rate, m^3/s
ε = turbulent kinetic energy dissipation rate, m^2/s^3
λ = geometric parameter in the zoning

Literature Cited

1. Patterson GK. *Simulating turbulent field mixers and reactors-or-taking the art out of the design*. In: Brodkey RS, editor. *Turbulence in Mixing Operations*. New York: Academic Press, 1975.
2. Fořt I, Obeid A, Březina V. Flow of liquid in a cylindrical vessel with a turbine impeller and radial baffles. *Collect Czech Chem Commun*. 1980;47:226–239.
3. Mann R, Hackett LA. Fundamentals of gas-liquid mixing in a stirred vessel: an analysis using networks of backmixed zones. In: Proceedings of the Sixth European Conference on Mixing. Pavia: BHRA, 1988:321–328.
4. Bourne JR, Yu S. Investigation of micromixing in stirred tank reactors using parallel reactions. *Ind Eng Chem Res*. 1994;33:41–55.
5. Alopaeus V, Koskinen J, Keskinen KI. Simulation of the population balances for liquid-liquid systems in a nonideal stirred tank, Part 1: Description and qualitative validation of the model. *Chem Eng Sci*. 1999;54:5887–5899.
6. Alopaeus V, Koskinen J, Keskinen KI, Majander J. Simulation of the population balances for liquid-liquid systems in a nonideal

stirred tank, Part 2: Parameter fitting and the use of the multiblock model for dense dispersions. *Chem Eng Sci*. 2002;57:1815–1825.
7. Rigopoulos S, Jones A. A hybrid CFD-reaction engineering framework for multiphase reactor modelling: basic concept and application to bubble column reactors. *Chem Eng Sci*. 2003;58:3077–3089.
8. Bezzo F, Macchietto S, Pantelides CC. A general methodology for hybrid multizonal/CFD models. I. Theoretical framework. *Comput Chem Eng*. 2004;28:501–511.
9. Laakkonen M, Alopaeus V, Aittamaa J. Validation of bubble breakage, coalescence and mass transfer models for gas-liquid dispersion in agitated vessel. *Chem Eng Sci*. 2006;61:218–228.
10. Kagoshima M, Mann R. Development of a networks-of-zones fluid mixing model for an unbaffled stirred vessel used for precipitation. *Chem Eng Sci*. 2006;61:2852–2863.
11. Harnby N, Edwards MF, Nienow AW. *Mixing in the Process Industries*, 2nd ed. London: Butterworth-Heinemann, 1992.
12. Perry RH, Green DW, Maloney JO. *Perry's Chemical Engineering Handbook*, 7th ed. New York: McGraw-Hill, 1997.
13. Paul EL, Atiemo-Obeng VA, Kresta SM, editors. *Handbook of Industrial Mixing*. Hoboken, NJ: Wiley, 2004.
14. Baldyga J, Podgorska W, Pohorecki R. Mixing-precipitation model with application to double feed semibatch precipitation. *Chem Eng Sci*. 1995;50:1281–1300.
15. Alexopoulos AH, Maggioris D, Kiparissides C. CFD analysis of turbulence non-homogeneity in mixing vessels. A two-compartment model. *Chem Eng Sci*. 2002;57:1735–1752.
16. Moilanen P, Laakkonen M, Visuri O, Alopaeus V, Aittamaa J. Modelling mass transfer in an aerated 0.2 m^3 vessel agitated by rushton, phasejet and combijet impellers. *Chem Eng J*. 2008;142:95–108.
17. Laakkonen M, Moilanen P, Alopaeus V, Aittamaa J. Dynamic modeling of local reaction conditions in an agitated aerobic fermenter. *AIChE J*. 2006;52:1673–1689.
18. Laakkonen M, Moilanen P, Alopaeus V, Aittamaa J. Modelling local gas-liquid mass transfer in agitated vessels. *Chem Eng Res Des*. 2007;85A5:665–675.
19. Moilanen P, Laakkonen M, Visuri O, Aittamaa J. Modelling local gas-liquid mass transfer in agitated viscous shear-thinning dispersions with CFD. *Ind Eng Chem Res*. 2007;46:7289–7299.
20. Galindo E. Aspects of the process for xanthan production. *Chem Eng Res Des*. 1994;72A:227–237.
21. Amanullah A, Hjorth SA, Nienow AW. A new mathematical model to predict cavern diameters in highly shear thinning, power law liquids using axial flow impellers. *Chem Eng Sci*. 1998;53:455–469.

Manuscript received Sept. 18, 2008, and revision received Jan. 9, 2009.